

## Biomimetic Nanofibrous Scaffolds: Preparation and Characterization of PGA/Chitin Blend Nanofibers

Ko Eun Park,<sup>†</sup> Hyun Ki Kang,<sup>‡</sup> Seung Jin Lee,<sup>§</sup> Byung-Moo Min,<sup>\*,‡</sup> and Won Ho Park<sup>\*,†</sup>

*Department of Textile Engineering, Chungnam National University, Daejeon 305-764, South Korea, Department of Oral Biochemistry and Craniomaxillofacial Reconstructive Science, Dental Research Institute, and BK21 HLS, Seoul National University College of Dentistry, Seoul 110-749, South Korea, and College of Pharmacy, Ewha Womans University, Seoul 120-750, South Korea*

*Received December 5, 2005*

Electrospinning of poly(glycolic acid) (PGA)/chitin blend solutions in 1,1,1,3,3,3-hexafluoro-2-propanol was investigated to fabricate biodegradable and biomimetic nanostructured scaffolds for tissue engineering. The morphology of the electrospun PGA/chitin blend nanofibers was investigated with a field emission scanning electron microscope. The PGA/chitin blend fibers have average diameters of around 140 nm, and their diameters have a distribution in the range 50–350 nm. The miscibility of PGA/chitin blend fibers was examined by differential scanning calorimetry. The PGA and chitin were immiscible in the as-spun nanofibrous structure. An in vitro degradation study of PGA/chitin blend nanofibers was conducted in phosphate-buffered saline, pH 7.2. It was found that the hydrolytic cleavage of PGA in the blend nanofibers was accelerated by the coexistence of hydrophilic chitin. To assay the cytocompatibility and cell behavior on the PGA/chitin blend nanofibrous scaffolds, cell attachment and spreading of normal human epidermal fibroblasts seeded on the scaffolds were studied. Our results indicate that the PGA/chitin blend nanofibrous matrix, particularly the one that contained 25% PGA and 75% chitin with bovine serum albumin coating, could be a good candidate for tissue engineering scaffolds, because it has an excellent cell attachment and spreading for normal human fibroblasts.

### 1. Introduction

Over the past decade, considerable efforts have attempted to develop scaffolds for tissue engineering, using biodegradable and biocompatible synthetic or natural polymers. Principally, the scaffold's design should mimic the structure and biological function of native extracellular matrix (ECM) proteins, which provide mechanical support and regulate cell activities. A nonwoven-type scaffold consisting of nanofibers is architecturally similar to the collagen structure of the ECM, in which collagen multi-fibrils of a nanofiber scale (50–500 nm) are composed of a three-dimensional network structure together with proteoglycans.<sup>1</sup> The scaffold texture, as well as the nature of the biomaterial, was also reported to control cell adhesion, proliferation, shape, and function.<sup>2–4</sup>

Recently, many researchers are trying to employ the electrospinning technique to prepare microporous biodegradable or biocompatible polymer scaffolds which are generally composed of nanosized fibers.<sup>5–12</sup> Li et al.<sup>6</sup> prepared poly(D,L-lactide-co-glycolide) ultrafine fibers that showed a morphological similarity to the ECM of natural tissue with a diameter range from 500 to 800 nm. Luu et al.<sup>7</sup> fabricated synthetic polymers (PLGA and PLA-PEO copolymer)/DNA composite scaffolds for therapeutic application in gene delivery for tissue engineering. Matthews

et al.<sup>8</sup> studied how electrospinning can be adapted to produce tissue-engineering scaffolds composed of collagen nanofibers (a matrix composed of 100 nm fiber). They found that the structural properties of electrospun collagen varied with the tissue of origin, the isotype, and the concentration of the collagen solution which was used to electrospin the fibers. Yoshimoto et al.<sup>9</sup> reported that the electrospun nonwoven poly( $\epsilon$ -caprolactone) could be a useful scaffold for bone tissue engineering.

As described previously, the natural ECMs in the body are mainly composed of collagen and proteoglycans whose compositions depend on tissue type. To establish an ideal scaffold mimicking the natural ECM, a nanofibrous structure composed of collagen and glycosaminoglycans (GAGs, main component of proteoglycans), such as chondroitin sulfates and hyaluronic acid, is desirable. However, the utility of collagen and GAGs has been limited by extremely high price and poor mechanical properties. Alternatively, the combination of synthetic and natural polymers, which could enhance biological interactions with cells and speed up tissue regeneration, should be considered as substitutes of ECM proteins.<sup>10</sup>

Until now, there have been several papers on electrospinning of biocompatible polymer blends. Most of them were mainly aimed at improving spinnability of natural polymers such as silk fibroin and chitosan.<sup>11–13</sup> Jin et al.<sup>11</sup> reported on the effect of poly(ethylene oxide) (PEO) on electrospinning of regenerated silk fibroin. They could fabricate porous silk fibroin scaffolds by removing PEO in the nanofibrous blend matrix, after crystallization of silk fibroin. Duan et al.<sup>12</sup> and Bhattarai et al.<sup>13</sup> also used PEO to improve the spinnability of chitosan. A nanofibrous blend matrix with higher PEO content swelled readily in water and completely lost its fibrous structure in a few days.<sup>12</sup> Although these recent efforts in fabricating biopolymer-based nanofibrous blend structures are encouraging, the

\* Corresponding authors: Byung-Moo Min, Department of Oral Biochemistry and Craniomaxillofacial Reconstructive Science, Seoul National University College of Dentistry, 28 Yeonkum-Dong, Chongno-Ku, Seoul 110-749, South Korea. Tel.: +82-2-740-8661. Fax: +82-2-740-8665. E-mail: bmmmin@snu.ac.kr. Won Ho Park, Department of Textile Engineering, Chungnam National University, Daejeon 305-764, South Korea. Tel.: +82-42-821-6613. Fax: +82-42-823-3736. E-mail: parkwh@cnu.ac.kr.

<sup>†</sup> Chungnam National University.

<sup>‡</sup> Seoul National University College of Dentistry.

<sup>§</sup> Ewha Womans University.

structural integrity in an aqueous environment (in vitro and in vivo) remains to be improved.

Among the biodegradable and biocompatible polymers, poly(lactic acid) (PLA), poly(glycolic acid) (PGA), and their copolymers have extensive applications to surgical sutures, implant materials, drug carriers, and scaffolds for tissue engineering. Chitin has structural characteristics similar to glycosaminoglycans (GAGs) such as chondroitin sulfates and hyaluronic acid in the ECM. It also has good biocompatibility and biodegradability, as well as various biofunctionalities including antithrombogenic, hemostatic immunity enhancing, and wound healing properties.<sup>14</sup> Chitin is more hydrophilic than PGA, and its biodegradation mechanism is significantly different from that of PGA. Chitin is degraded via the cleavage of the  $\beta$ -glycosidic linkage between *N*-acetylglucosamine units by an enzyme like lysozyme, while PGA is degraded via hydrolytic cleavage at ester bonds. Therefore, the PGA/chitin blends may be affected by their respective hydrophilicity and degradability.

In this study, the nanostructured scaffolds of PGA/chitin blends were produced via electrospinning to develop novel biodegradable and biomimetic scaffolds. The hydrolytic degradation behavior of PGA/chitin blend nanofibers was investigated in vitro. In addition, we examined the effect of PGA/chitin scaffolds on the cell attachment and spreading of normal human epidermal fibroblasts (NHEF).

## 2. Materials and Methods

**2.1. Materials.** PGA polymer (Mw = 14 000–20 000) was kindly supplied by Purac Co. The chitin from crab shells supplied by Kumho Chemical Co. (Korea) was partially depolymerized by  $\gamma$ -ray irradiation to improve its solubility.<sup>15</sup> The molecular weight (Mw) and degree of deacetylation (DD) of depolymerized chitin were 91 000 and 8%, respectively. 1,1,1,3,3,3-hexafluoro-2-propanol (HFIP) and phosphate-buffered saline (PBS) solution (pH 7.2) were purchased from Aldrich Co. and used as received.

**2.2. Viscosity Measurement.** The viscosity of PGA/chitin blend solutions (PGA/chitin = 100/0, 75/25, 50/50, 25/75, 0/100, w/w) in HFIP was determined with a Brookfield digital viscometer (model DV-E) at 25 °C.

**2.3. Electrospinning of PGA/chitin Blend Solutions.** PGA and chitin were dissolved in HFIP at concentration of 8 wt % and 5 wt %, respectively. A series of PGA/chitin blend solutions (PGA/chitin = 100/0, 75/25, 50/50, 25/75, 0/100, w/w) were prepared by mixing each solution at predetermined ratios and then electrospun under the same processing conditions. In the electrospinning process, a high electric potential was applied to a droplet of blend solution at the tip (ID, 0.495 mm) of a syringe needle. The electrospun blend nanofibers were collected on a target which was placed at a distance of 7 cm from the syringe tip. A voltage of 17 kV was applied to the collecting target by a high-voltage power supply (Chungpa EMT, CPS-40K03). Mass flow rate of solutions was 4 mL/h. All electrospinnings were carried out at room temperature.

**2.4. Field Emission Scanning Electron Microscopy (FE-SEM).** The morphology and pore structure of electrospun and degraded PGA/chitin blend fibers were observed by a field emission scanning electron microscope (FE-SEM, JSM-6335F, JEOL). Prior to the observation, platinum was coated by ion sputtering for a few seconds. The average diameter and diameter distribution were obtained by analyzing SEM images with a custom code image analysis program (Scope Eye II).

**2.5. Differential Scanning Calorimetry (DSC).** DSC measurements were conducted with a Perkin-Elmer DSC7 instrument in a nitrogen atmosphere. Approximately 10 mg samples were sealed in an aluminum pan for the measurements. The samples were heated from 10 to 250 °C at a rate of 20 °C/min, held at 250 °C for 1 min, and then quenched to 0 °C. The samples were reheated to 250 °C.

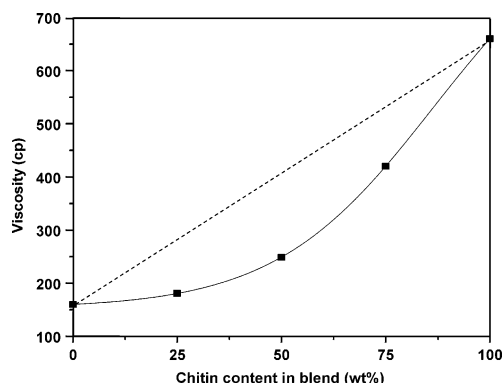


**Figure 1.** Changes in solution viscosity according to blend ratio of PGA/chitin.

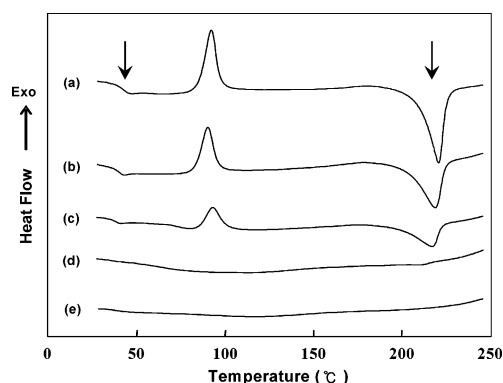


**Figure 2.** DSC thermograms of PGA/chitin blend nanofibers prepared by electrospinning: (a) pure PGA, (b) PGA/chitin (75/25), (c) PGA/chitin (50/50), (d) PGA/chitin (25/75), and (e) pure chitin.

**2.6. X-ray Diffraction.** The crystalline structure of the samples was analyzed on a wide-angle X-ray diffractometer (model D/max-IIB, Rigaku International Corp.).

**2.7. Water Uptake Capacity of PGA/Chitin Blend Nanofibers.** The water uptake capacity of PGA/chitin blend nanofibers (200 mg) was determined by immersing the fibers in distilled water for 1 h at room temperature.<sup>16</sup> The hydrated samples were taken and immediately weighed after removing the surface water with a filter paper. The water content (WC, %) was calculated as follows:

$$\text{WC (\%)} = (W - W_0)/W_0 \times 100$$

$W$  and  $W_0$  denote the weight of sample before and after immersion in water for 1 h, respectively.

**2.8. In Vitro Degradation.** PGA/chitin blend scaffolds were cut into a rectangular shape with dimensions of  $40 \times 40 \times 0.1$  mm<sup>3</sup> for the degradation test. The specimens were placed in closed bottles containing 50 mL of PBS (pH 7.2) and incubated at a temperature of 37 °C for different periods of time up to 45 days. After each degradation period, the specimen was washed with distilled water and dried in a vacuum oven at room temperature for 24 h. The weight loss percentages of the specimens were calculated from the weights obtained before and after degradation.

**2.9. Cells and Cell Culture.** Primary NHEF were prepared and maintained, as previously reported.<sup>17</sup> The tissue samples were obtained from human foreskins of patients (1 to 3 years of age) undergoing surgery. Briefly, samples were thoroughly washed with calcium- and magnesium-free Hanks' balanced salt solution (Invitrogen, Carlsbad, CA). Primary NHEF were established from explant cultures of foreskin. When the cells reached 80% confluence, they were serially subcultured, being passaged at every 80% confluence level, and the fourth passage fibroblasts were used in the described experiments. The cells were cultured in Dulbecco's modified Eagle's medium (Sigma-Aldrich, Saint Louis, MO), supplemented with 10% fetal bovine serum.

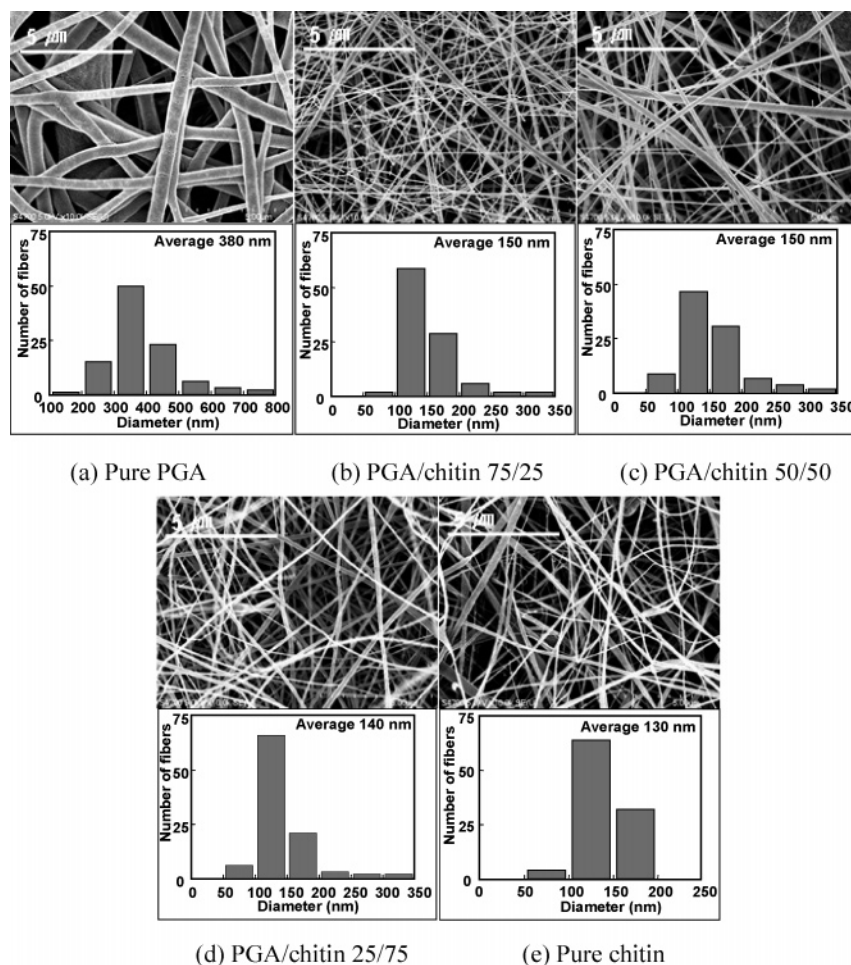


**Figure 3.** SEM micrographs of PGA/chitin blend nanofibers.

**2.10. Cell Attachment and Spreading Assays.** Cell attachment was assayed using a modification of the method of Mould et al.<sup>18</sup> Briefly, PGA/chitin blend nanofibrous matrixes were cut out with a punch (14 mm in diameter) and put onto the 24-well culture plates (Nunc, Denmark). There are two methods for pretreatment of PGA/chitin blend nanofibrous matrixes. One way is 24-well culture plates containing PGA/chitin blend scaffolds being soaked in serum-free medium, and the other is coating with PBS containing 0.1% heat-inactivated bovine serum albumin (BSA; Sigma), both methods for 1 h at room temperature. The plates were then rinsed with PBS. Cells were detached by treatment with 0.05% trypsin and 0.53 mM ethylenediaminetetraacetic acid in PBS, resuspended in the culture media, added to each plate ( $5.3 \times 10^4$  cells/cm<sup>2</sup>), and incubated for 1 h at 37 °C. Unattached cells were removed by rinsing twice with PBS. Attached cells were fixed with 10% formalin in PBS for 15 min and rinsed twice with PBS. Cells attached to the PGA/chitin blend nanofibrous matrixes were stained with hematoxylin and eosin. The wells were gently rinsed 3 times with double distilled water. The PGA/chitin blend nanofibrous matrixes were mounted, and cells attached onto the nanofibers were photographed. To ensure a representative count, each nanofiber sample was divided into quarters, and two fields per quarter were photographed with an Olympus BX51 microscope at 100 $\times$ .

Cell spreading was analyzed using photographs of the cell attachment assay. To ensure a representative count, each nanofiber sample was divided into quarters, and two fields per quarter were photographed with an Olympus BX51 microscope at 100 $\times$ . Cells that adopted a flattened, polygonal shape with filopodia- and lamellipodia-like extensions were regarded as spreading cells. In contrast, cells that resisted washing and remained tethered to the plate surface were regarded as nonspreading cells. The percentage of cells displaying spread morphology was quantified by dividing the number of spread cells by the total number of bound cells.

**2.11. Statistics and Data Analysis.** Cell attachment and spreading onto the PGA/chitin blend nanofibers were compared by analysis of variance (ANOVA), using the STATISTICA 6.0 software package. When significant differences were found, pairwise comparisons were performed using Scheffe's adjustment. Differences were considered statistically significant for  $P$  values < 0.05.

### 3. Results and Discussion

**3.1. Morphology of PGA/Chitin Blend Nanofibers.** To mimic the nanofibrous assembled structure of ECM, we chose PGA and chitin as substitutes of collagen and GAGs in the ECM, respectively. Figure 1 shows change in solution viscosity according to the blend ratio. The solution viscosities of PGA (8 wt %) and chitin (5 wt %) were 160 and 660 cP, respectively. The viscosities of blend solutions were slightly lower than expected by the additive rule (dotted line), indicating a negligible interaction between PGA and chitin in blend solutions. Therefore, we can expect to observe significantly phase separated morphology from electrospun blend nanofibers. One of the most effective methods for determining the miscibility between blend pairs is by measuring the thermal properties of polymer blends.<sup>19</sup> When blend pairs are miscible at the molecular level, a single, composition-dependent  $T_g$  between the  $T_g$ 's of the blend components is observed. Figure 2 shows the DSC thermograms of the PGA/chitin blend nanofibers prepared by electrospinning. For as-spun samples, the  $T_g$  and  $T_m$  values of PGA did not change, irrespective of blend composition. The results clearly show that the blend fibers of PGA and chitin were immiscible in the as-spun state. The solubility parameters ( $\delta$ ) of PGA and



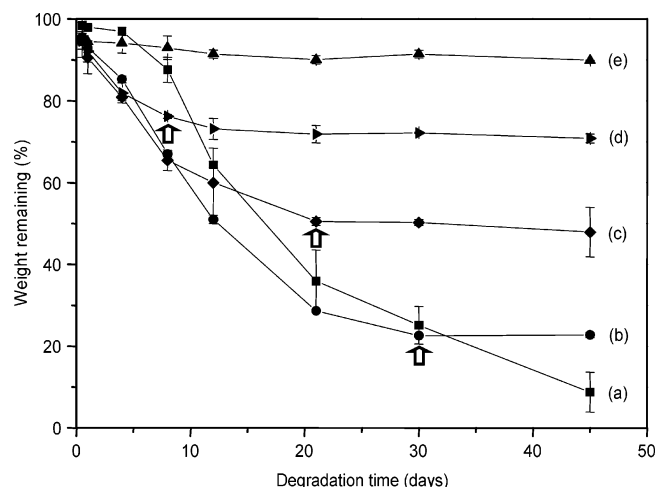
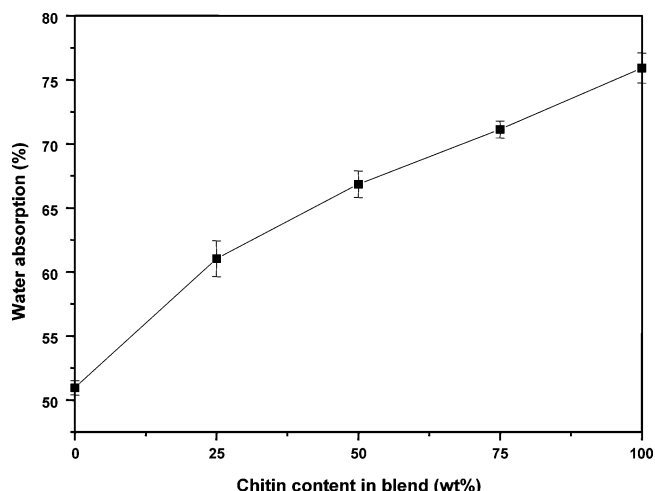


**Figure 4.** Weight remaining (%) of PGA/chitin blend nanofibers according to the degradation time up to 45 days: (a) pure PGA, (b) PGA/chitin (75/25), (c) PGA/chitin (50/50), (d) PGA/chitin (25/75), and (e) pure chitin. Arrow indicates the time to ultimate degradation value.

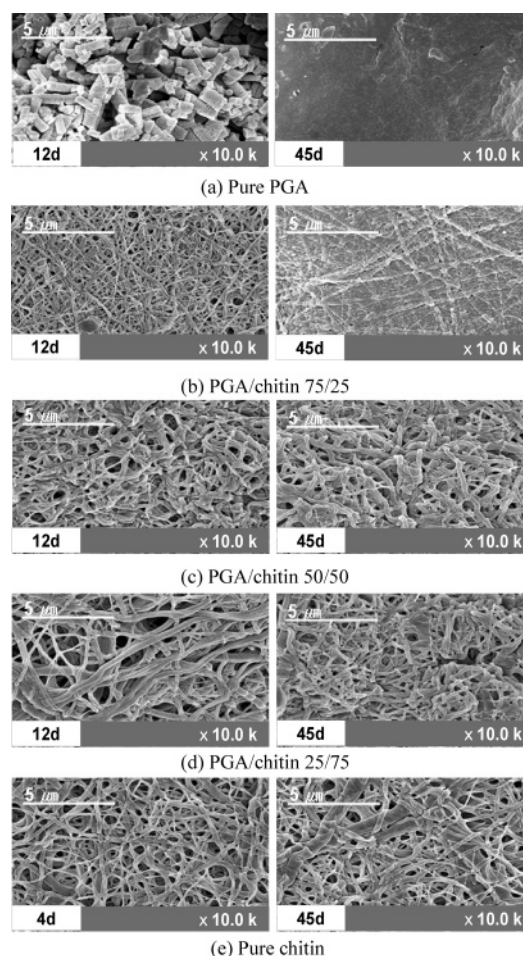
chitin were 34.0 and 17.8 J<sup>1/2</sup>/cm<sup>3/2</sup>, respectively.<sup>20</sup> The difference in the  $\delta$  values of PGA and chitin leads to immiscibility.

Figure 3 shows SEM micrographs of the blend nanofibers composed of PGA and chitin. As shown in Figure 3a and e, pure PGA nanofibers had a higher average diameter and broader distribution than pure chitin nanofibers, although the viscosity (660 cP) of the chitin solution was higher than that (160 cP) of the PGA solution. This indicates that the nature of polymer plays an important role in determining the diameter of electrospun nanofibers. PGA has a relatively hydrophobic character, compared with chitin. Generally, it is known that the electrospinning of polymers with higher polarity provides nanofibrous products with smaller diameters. The PGA/chitin blend fibers had similar average diameters (~150 nm) but slightly broader distribution in the range 50–350 nm, compared to pure chitin fibers.

**3.2. In Vitro Degradation Behavior of PGA/Chitin Blend Nanofibers.** Figure 4 shows the weight remaining (%) of PGA/chitin blend nanofibers according to the degradation time up to 45 days. The weight loss of pure PGA nanofibers was above 90% after 45 days. As expected, the ultimate weight loss of blend fibers after 45 days decreased with an increase in the chitin content in blends and was similar to the PGA content in blend fibers, because chitin was not degraded in PBS solution. This indicates that the PGA component in blend fibers was almost degraded during the 45 days. Interestingly, the degradation rates of PGA/chitin blend fibers in the early days were much faster than for pure PGA fibers. Among the PGA/chitin blends, the degradation rate also increased with the increase in hydrophilic chitin content. As the content of chitin in blend fibers increased from 25% to 75%, the times to ultimate degradation value (referring to arrows) were decreased from 30 days to 13 days. This suggests that the hydrolysis of PGA could be accelerated by blending with chitin. This accelerating effect might be caused by the hydrophilicity of chitin and the difference in fiber size. The degradation of PGA proceeds via hydrolytic cleavage of the ester bond in polymer backbone. The degradation rate strongly depends on the accessibility of water to ester bonds. Accordingly, the degradation rate of the dispersed PGA phase is mainly determined by the hydrophilicity and crystallinity of the PGA/chitin blend fibers. PGA has a relatively hydrophobic character and a high degree of crystallinity, as well as higher fiber diameter, while chitin is more hydrophilic and semicrys-



**Figure 5.** Water content of PGA/chitin blend fibers with different chitin contents.



**Figure 6.** Morphological changes of PGA/chitin blend nanofibers at 12 and 45 days of degradation.

talline. Blending of chitin with PGA is expected to produce different degrees of matrix hydration depending on the blend ratio.

To investigate the effect of hydration on degradation rate of PGA, we measured the water content of PGA/chitin blend nanofibers. Figure 5 shows the water content of PGA/chitin blend fibers with different chitin contents. The water content increased with an increase in the amount of chitin in blends. The hydrolytic chain scission of PGA is proportional to the amount of absorbed water and ester bonds. When PGA is

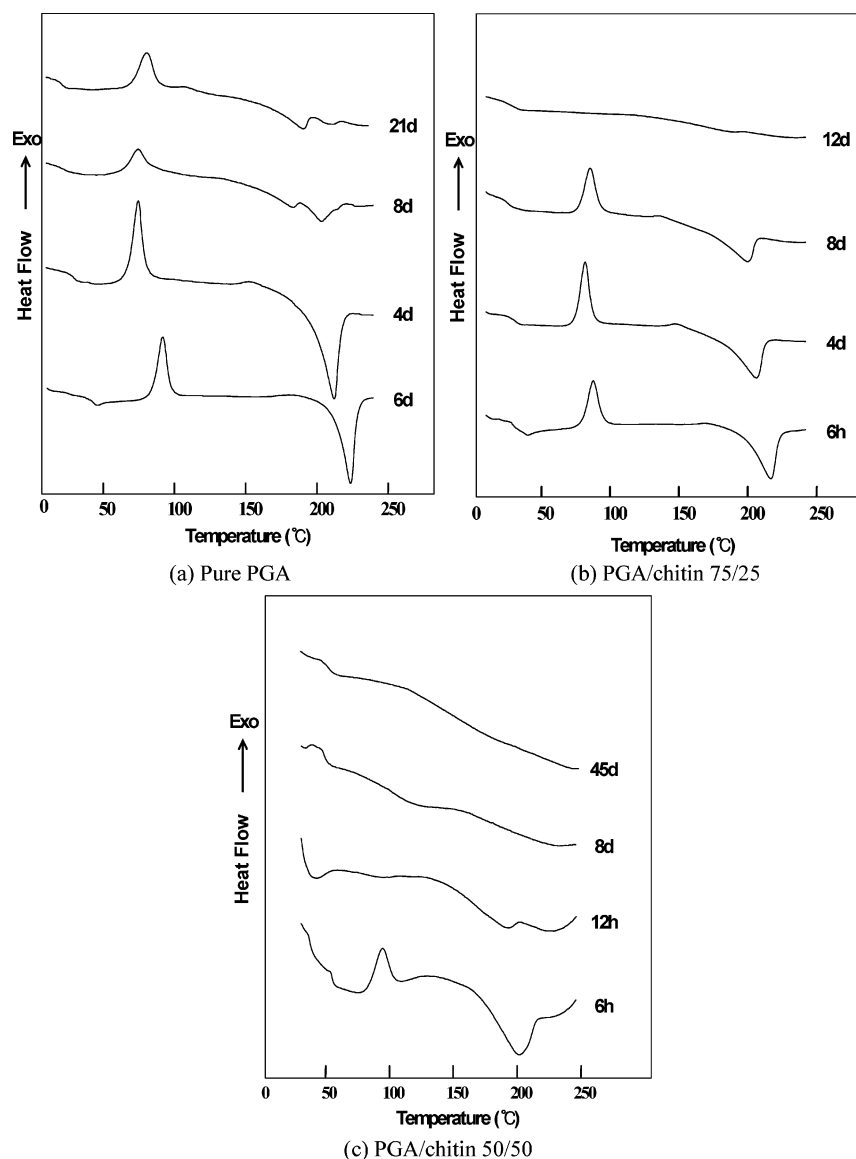
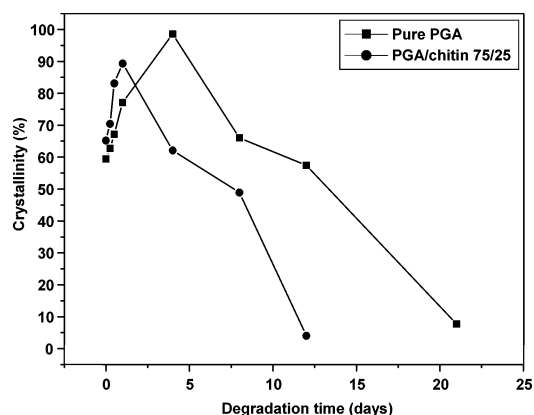


**Figure 7.** Changes in thermal properties of PGA/chitin blend fibers during in vitro degradation.

blended with a hydrophilic chitin, it is expected to bring about a rapid increase in the PGA hydrolysis rate due to the higher water absorption ability. This indicates that chitin has an important role in accelerating the degradation of PGA molecules.

Figure 6 illustrates the morphological changes of electrospun PGA/chitin blend nanofibers at 12 and 45 days of degradation. After 12 days, pure PGA fibers were broken down into short fiber fragments (Figure 6a, left). On the contrary, pure chitin and PGA/chitin blend fibers were somewhat swollen, but no significant morphological change was observed at 12 days. (Figure 6b–e, left). After 45 days, pure PGA and PGA/chitin (75/25) showed a trace of membrane-like structure (Figure 7a,b, right). However, no significant morphological change in nanofibrous structure was observed for pure chitin fibers and the PGA/chitin blend fibers with chitin contents of above 50%, after 45 days (Figure 7c–e, right).

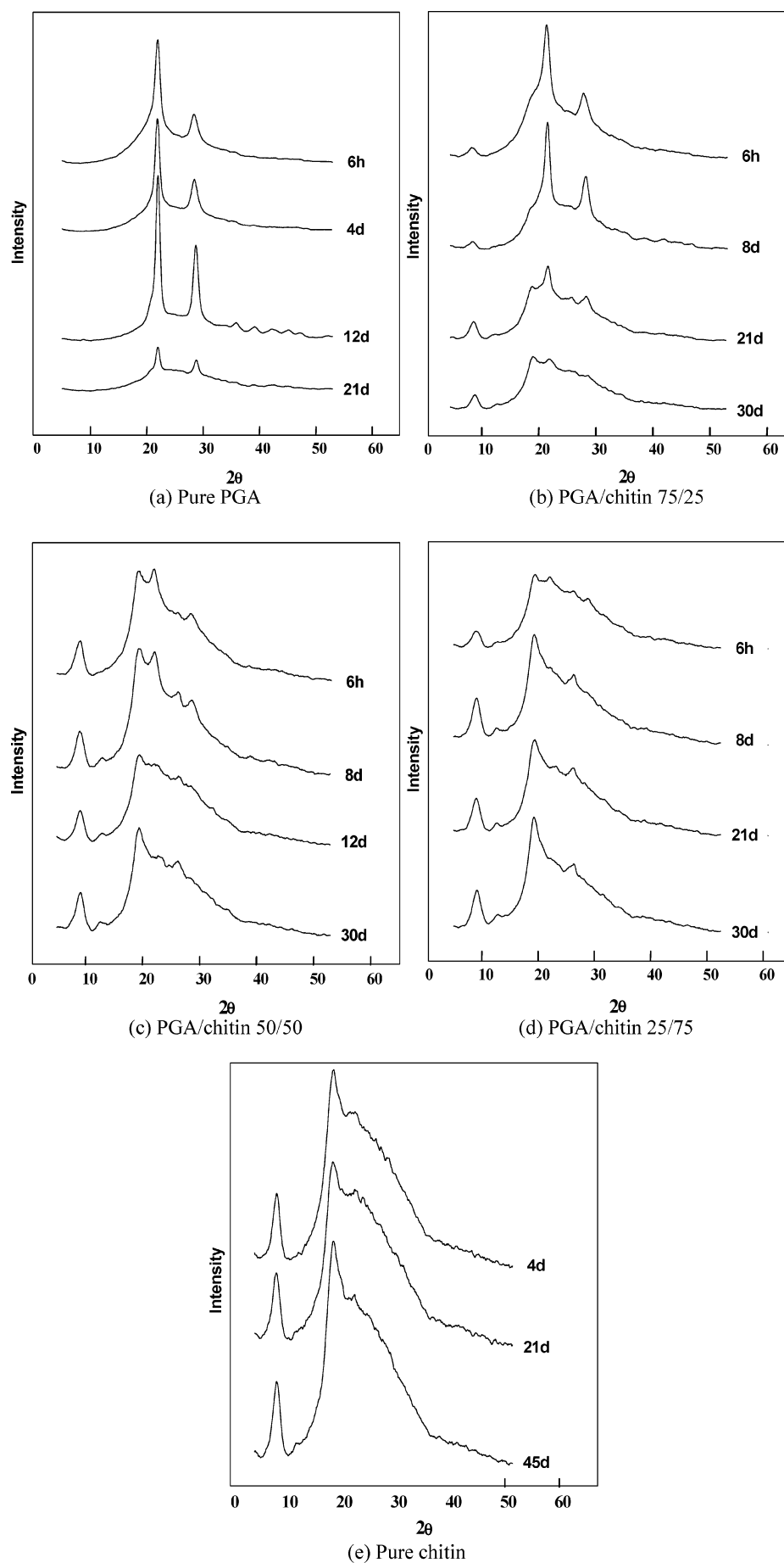
Figure 7 shows the changes in thermal properties of PGA/chitin blend fibers during in vitro degradation. In our previous study, the crystallinity of PGA nanofibers was first increased by the cleavage-induced crystallization and then gradually decreased during in vitro degradation.<sup>21</sup> In the case of PGA/chitin (75/25), the melting endotherm of PGA (~220 °C) became weaker and broader after 8 days as the degradation in



**Figure 8.** Changes in crystallinity (%) of pure PGA and PGA/chitin (75/25) blend fibers during in vitro degradation.

crystalline regions of PGA started. The melting endotherm of PGA, in PGA/chitin (50/50) blend fibers, almost disappeared at 8 days.

Figure 8 shows the changes in the crystallinity (%) of pure PGA and PGA/chitin (75/25) blend fibers during degradation. The crystallinity (%) was determined from the melting enthalpy with heat of fusion of 139 J/g for PGA.<sup>22</sup> A large increase in

**Figure 9.** Changes in WAXD patterns of PGA/chitin blend fibers during in vitro degradation.

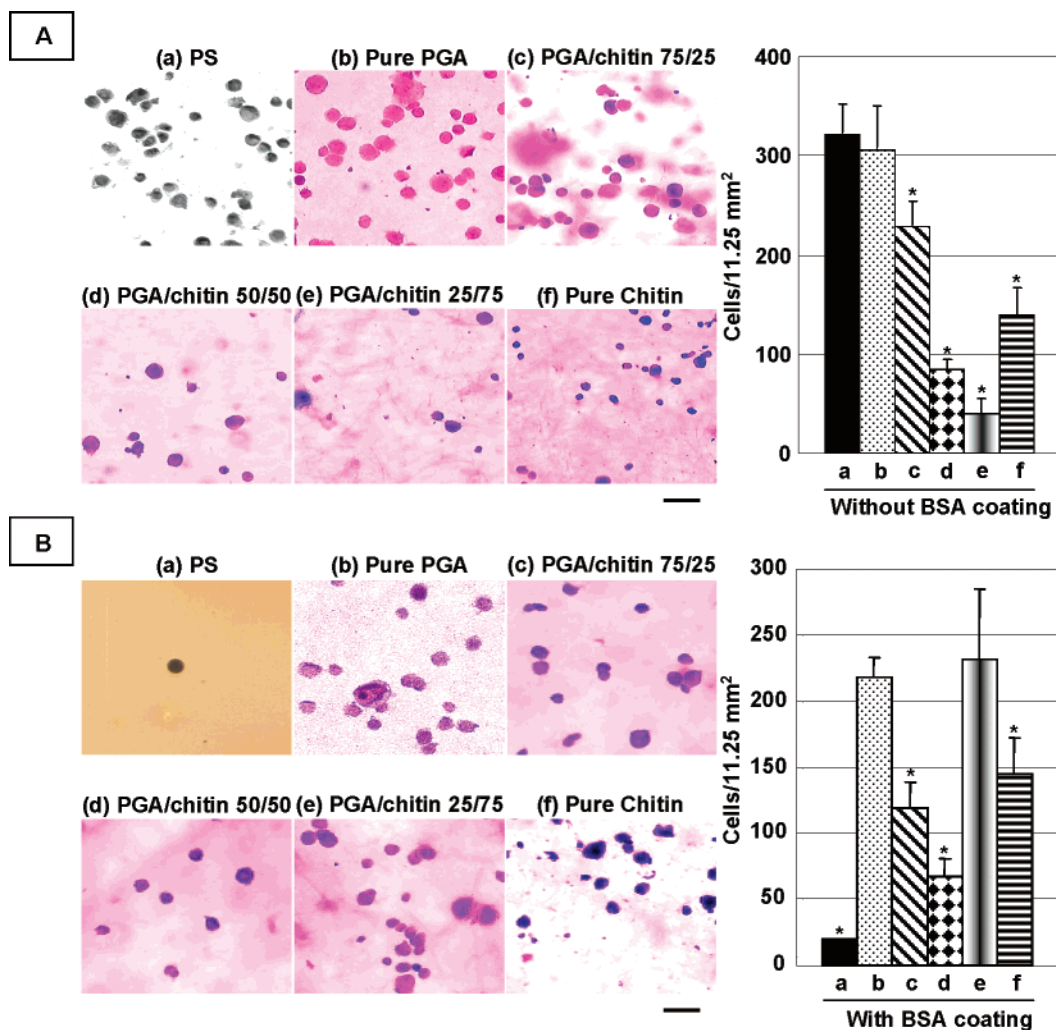


**Figure 10.** Cell attachment of proliferating NHEF plated onto PGA/chitin blend nanofibrous matrices. Microphotographs and level of cell attachment of cultured cells onto PGA/chitin blend nanofibrous matrices without (A) or with (B) BSA coating. Data are expressed as mean  $\pm$  SD ( $n = 4$ ). ANOVA:  $P < 0.05$ . Pairwise comparisons: \* $P < 0.05$  vs pure PGA nanofibers. (a) polystyrene surface, (b) pure PGA, (c) PGA/chitin (75/25), (d) PGA/chitin (50/50), (e) PGA/chitin (25/75), and (f) pure chitin. Bar, 100  $\mu$ m.

the crystallinity for pure PGA fibers was observed within the first 4 days, and thereafter, the crystallinity gradually decreased up to the later days. In the PGA/chitin (75/25) blend nanofibers, the crystallinity of the PGA component increased up to 1 day and subsequently decreased. Also, the crystallinity in the PGA/chitin (75/25) blend reached almost 0% at 12 days, whereas the crystallinity in pure PGA was about 60% at the same period. This indicates that the degradation rate of PGA in PGA/chitin blends was much faster than that of pure PGA and thus accelerated by blending with chitin.

Figure 9 shows the WAXD patterns of PGA/chitin blend fibers during in vitro degradation. For pure PGA and PGA/chitin (75/25) blend fibers, the characteristic WAXD peaks for PGA at  $22^\circ$  and  $29^\circ$  were clearly observed, which were assigned to (110) and (020) planes, respectively.<sup>23</sup> In case of PGA/chitin (50/50) and (25/75) fibers, the diffraction peaks at  $\sim 8^\circ$  and  $\sim 19^\circ$ , which correspond to the most distinctive peak for crystalline chitin, appeared and became stronger because of selective degradation of the PGA component, according to the degradation time. However, no significant changes in the WAXD patterns of pure chitin nanofibers were observed up to 45 days, because the degradation of chitin was negligible.

**3.3. Attachment and Spreading of Normal Human Fibroblasts on PGA/Chitin Blend Nanofibers with or without BSA Coating.** It is interesting to study the cytocompatibility of the

PGA/chitin blend nanofibers with or without BSA coating, in relation with a possible use as wound dressing materials and scaffolds for tissue engineering. Moreover, since the connective tissue plays an important role in reconstructing skin defects, the response of normal human fibroblasts forming these tissues was analyzed in vitro. Since the absence of cytotoxicity of PGA and chitin has already been demonstrated,<sup>24–26</sup> and initial cell attachment and spreading might be an important contributing factor to their potential use as wound dressings and scaffolds for tissue engineering, the initial cell attachment and spreading on these PGA/chitin blend scaffolds were studied. To assess cell attachment and spreading, PGA/chitin blend nanofibrous scaffolds that were pretreated with or without BSA were seeded with normal human fibroblasts. The attachment of the cultured cells was evaluated using the cell attachment assay in serum-free medium. The purpose of soaking of scaffolds, absent of BSA, with serum-free medium is to observe and compare the biological properties of PGA/chitin blend nanofibrous scaffolds. In contrast, the purpose of the BSA coating is to imitate the adsorption of blood proteins. Exponentially proliferating NHEF adherent to the PGA/chitin blend nanofibrous scaffolds were microphotographed in the attachment assay after washing, fixing, and staining the cells with hematoxylin and eosin.

Figure 10A shows representative microscopic fields for cells adhering on PGA/chitin blend nanofibrous scaffolds only,



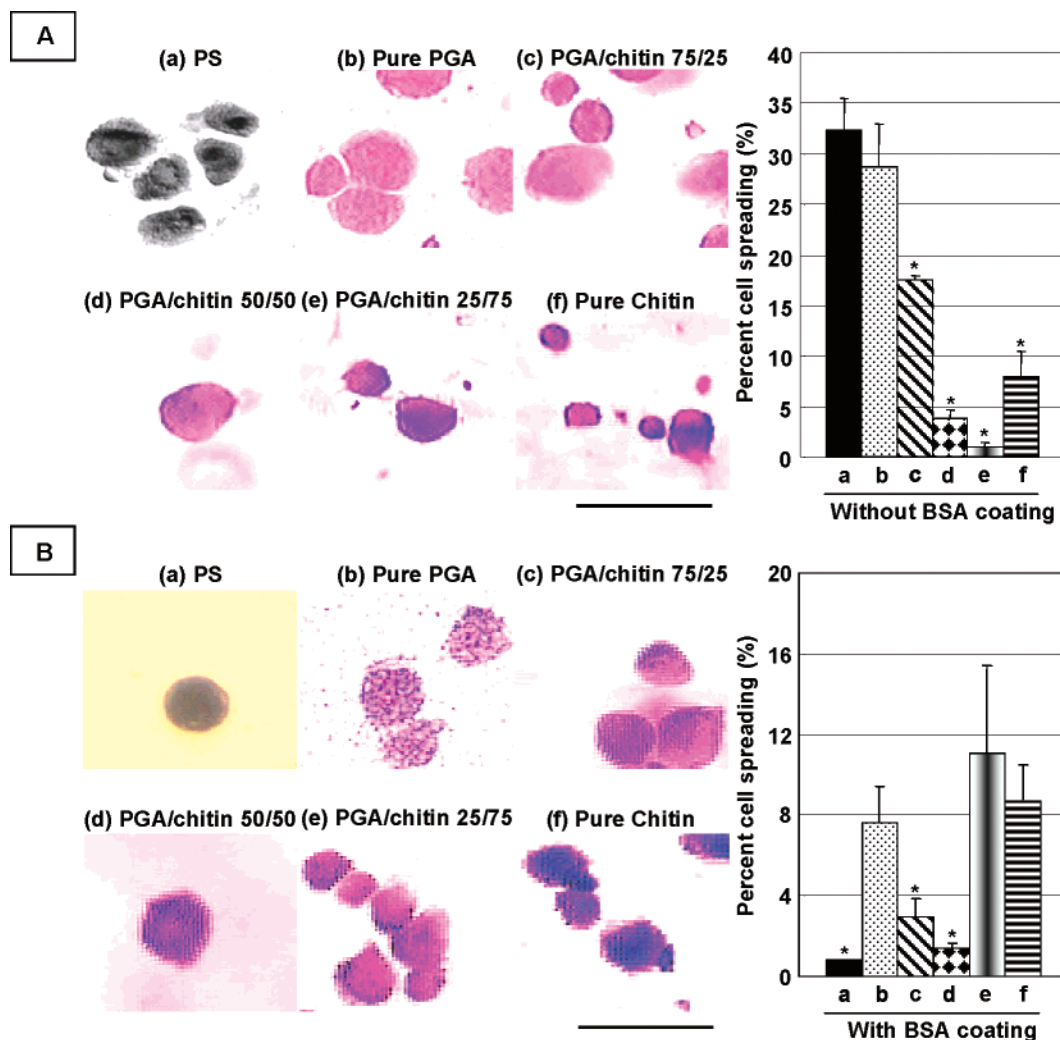


**Figure 11.** Cell spreading of proliferating NHEF plated onto PGA/chitin blend nanofibrous matrixes. Microphotographs and incidence of cultured cells spreading onto PGA/chitin blend nanofibrous matrixes without (A) or with (B) BSA coating. Data are expressed as mean  $\pm$  SD ( $n = 4$ ). ANOVA:  $P < 0.05$ . Pairwise comparisons: \* $P < 0.05$  vs pure PGA nanofibers. (a) polystyrene surface, (b) pure PGA, (c) PGA/chitin (75/25), (d) PGA/chitin (50/50), (e) PGA/chitin (25/75), and (f) pure chitin. Bar, 100  $\mu$ m.

without coated BSA. Relatively high cell attachment was observed on polystyrene surfaces for NHEF. The number of adhering cells observed on the pure PGA scaffolds alone was very similar to that of the polystyrene surface. As the PGA content in blend scaffolds decreased from 100%, 75%, 50%, to 25%, the adhesion activity profile onto the PGA/chitin blend nanofibrous scaffolds gradually decreased, indicating that PGA accelerated cell attachment (Figure 10A). In addition, the attachment activity profile on the pure chitin scaffolds was higher than that on the PGA/chitin blend nanofibers that contained less than 50% PGA, but lower than the PGA/chitin blend nanofibers that contained more than 75% PGA (Figure 10A). To imitate the adsorption of blood proteins when wound dressing materials and scaffolds for tissue engineering were applied to wounds, the PGA/chitin blend nanofibrous scaffolds were coated with 0.1% BSA prior to determining cell attachment activity. Extremely low cell attachment was observed on BSA-coated polystyrene surfaces for NHEF (Figure 10B). In contrast, relatively high cell attachment was observed on BSA-coated pure PGA scaffolds alone for NHEF. When the attachment activity profile on the pure PGA scaffolds alone with or without BSA coating was compared with each other, cell attachment onto the PGA sample without BSA coating was better than that of the PGA sample with BSA coating for NHEF (Figure 10A and B). As the PGA content in matrixes decreased from 100%,

75%, to 50%, the attachment activity profile on the PGA/chitin blend nanofibrous scaffolds gradually decreased. However, PGA/chitin blend nanofibrous scaffolds, containing 25% PGA and coated with BSA, showed relatively high cell attachment activity and slightly exceeded the pure PGA scaffolds, but were statistically insignificant. Similarly, the attachment activity profile onto the original chitin scaffolds with BSA coating was higher than that of the PGA/chitin blend nanofibrous scaffolds that contained either 75% or 50% PGA with BSA coating, but lower than that of the pure PGA scaffolds only (Figure 10B). Although PGA/chitin blend nanofibrous scaffolds that contained 25% PGA without BSA coating showed very low cell attachment activity for normal human fibroblasts, the scaffolds with BSA coating had the highest cell attachment activity under our experimental conditions. These results indicate that PGA scaffolds, with or without BSA coating, and PGA/chitin blend nanofibrous scaffolds, containing 25% PGA and BSA coating, are functionally active in terms of cell attachment for normal human fibroblasts.

To further evaluate the effects of BSA coating on cell attachment, we determined whether adherent cells were tethered to the substrate or spread over the substrate. Photographs of exponentially proliferating NHEF adherent to PGA/chitin blend nanofibrous scaffolds with or without BSA coating were taken in the attachment assay. Interestingly, cell spreading and cell



attachment, which were observed on PGA/chitin blend nanofibrous scaffolds with or without BSA coating, showed similar patterns in the graphs. In the case of without BSA coating, as the PGA content in blend scaffolds decreased from 100%, 75%, 50%, to 25%, the spreading profile onto the PGA/chitin blend nanofibrous scaffolds gradually decreased, indicating that the PGA also accelerated cell spreading (Figure 11A). However, the scaffolds with BSA coating showed a different result: as the PGA content decreased from 100%, 75%, to 50%, the spreading profile onto the PGA/chitin blend nanofibrous scaffolds gradually decreased, but the one with 25% PGA showed the highest spreading profile out of the BSA coating group. These results indicate that PGA/chitin blend nanofibrous scaffolds, containing 25% PGA and 75% chitin, could be a good candidate for cell attachment and spreading of normal human fibroblasts, particularly in its application on skin wounds.

#### 4. Conclusions

To mimic the natural ECM, PGA/chitin blend nanofibrous scaffolds were obtained by electrospinning with the average fiber diameter in the range 130–150 nm, whereas electrospinning of pure chitin produced an average fiber diameter of 380 nm. Electrospinning of PGA/chitin blend solutions produced blend nanofibers with phase-separated structure, because PGA and chitin were immiscible in the as-spun fibrous structure. From in vitro degradation results, it was found that PGA in PGA/chitin blend nanofibers were degraded faster than pure PGA nanofibers. This accelerating effect may be attributed to the hydrophilicity of chitin.

The cell attachment and spreading onto the PGA/chitin blend nanofibrous scaffolds showed relatively promising results for the normal human fibroblasts tested. The PGA/chitin blend matrix, particularly the one that contained 25% PGA and 75% chitin with BSA coating, could be a good candidate for tissue engineering scaffolds, because it has both biomimetic three-dimensional structure, resembling the collagen-GAGs composite structure in the ECM, and an excellent cell attachment and spreading for normal human fibroblasts.

**Acknowledgment.** This work was supported by the Ministry of Commerce, Industry and Energy (Korea).

#### References and Notes

- (1) Nishido, T.; Yasumoto, K.; Otori, T.; Desaki, J. *Invest. Ophthalmol. Visual Sci.* **1988**, *29*, 1887–1890.
- (2) Chen, C. S.; Mrksich, M.; Huang, S.; Whitesides, G. M.; Ingber, D. E. *Science* **1997**, *276*, 1425–1428.
- (3) Patel, N.; Padera, R.; Sanders, G. H. W.; Cannizzaro, S. M.; Davies, M. C.; Langer, R.; Roberts, C. J.; Tendler, S. J. B.; Williams, P. M.; Shakesheff, K. M. *FASEB J.* **1998**, *12*, 1447–1454.
- (4) van Kooten, T. G.; Whitesides, J. F.; von Recum, A. F. *J. Biomed. Mater. Res.* **1998**, *43*, 1–14.
- (5) Kenawy, E. R.; Layman, J. M.; Watkins, J. R.; Bowlin, G. L.; Matthews, J. A.; Simpson, D. G.; Wnek, G. E. *Biomaterials* **2003**, *24*, 907–913.
- (6) Li, W. J.; Laurencin, C. T.; Caterson, E. J.; Tuan, R. S.; Ko, F. K. *J. Biomed. Mater. Res.* **2002**, *60*, 613–621.
- (7) Luu, Y. K.; Kim, K.; Hsiao, B. S.; Chu, B.; Hadjiargyrou, M. *J. Controlled Release* **2003**, *89*, 341–353.
- (8) Matthews, J. A.; Wnek, G. E.; Simpson, D. G.; Bowlin, G. L. *Biomacromolecules* **2002**, *3*, 232–238.
- (9) Yoshimoto, H.; Shin, Y. M.; Terai, H.; Vacanti, J. P. *Biomaterials* **2003**, *24*, 2077–2082.
- (10) Zhanng, Y.; Ouyang, H.; Lim, C. T.; Ramakrishna, S. *J. Biomed. Mater. Res. B* **2005**, *72*, 156–165.
- (11) Jin, H. J.; Fridrikh, S. V.; Rutledge, G. C.; Kaplan, D. L. *Biomacromolecules* **2002**, *3*, 1233–1239.
- (12) Duan, B.; Dong, C. H.; Yuan, X. Y.; Yao, K. D. *J. Biomater. Sci., Polym. Ed.* **2004**, *15*, 797–811.
- (13) Bhattarai, N.; Edmondson, D.; Veis, O.; Matsen, F. A.; Zhang, G. M. *Biomaterials* **2005**, *26*, 6176–6184.
- (14) Yusof, N. L. B. M.; Wee, A.; Lim, L. Y.; Khor, E. *J. Biomed. Mater. Res.* **2003**, *66*, 224–232.
- (15) Min, B. M.; Lee, S. W.; Lim, J. N.; You, Y.; Lee, T. S.; Kang, P. H.; Park, W. H. *Polymer* **2004**, *45*, 7137–72.
- (16) Mi, F. L.; Lin, Y. M.; Wu, Y. B.; Shyu, S. S.; Tsai, Y. H. *Biomaterials* **2002**, *23*, 3257–3267.
- (17) Min, B. M.; Lee, G.; Kim, S. H.; Nam, Y. S.; Lee, T. S.; Park, W. H. *Biomaterials* **2004**, *25*, 1289–1297.
- (18) Mould, A. P.; Askari, J. A.; Humphries, M. J. *J. Biol. Chem.* **2000**, *275*, 20324–20336.
- (19) Olabisi, O.; Robeson, L. M.; Shaw, M. T., Eds. *Polymer–Polymer Miscibility*; Academic Press: New York, 1979; pp 117–189.
- (20) Mi, F. L.; Shyu, S. S.; Lin, Y. M.; Wu, Y. B.; Peng, C. K.; Tsai, Y. H. *Biomaterials* **2003**, *24*, 5023–5036.
- (21) You, Y.; Min, B. M.; Lee, S. J.; Lee, T. S.; Park, W. H. *J. Appl. Polym. Sci.* **2005**, *95*, 193–200.
- (22) Shum, A. W. T.; Mak, A. F. T. *Polym. Degrad. Stab.* **2003**, *81*, 141–149.
- (23) Wang, Z. G.; Wang, X.; Hsiao, B. S.; Andjelic, S.; Jamiolkowski, D.; McDivitt, J. *Polymer* **2001**, *42*, 8965–8973.
- (24) Chow, K. S.; Khor, E. *Carbohydr. Polym.* **2002**, *47*, 357–363.
- (25) Ignatius, A. A.; Claes, L. E. *Biomaterials* **1996**, *17*, 831–839.
- (26) Zange, R.; Kissel, T. *Eur. J. Pharm. Biopharm.* **1997**, *44*, 149–157.

BM0509265